Advances in EXAFS Studies of Thermal Properties of Crystals

Paolo Fornasini

Dipartimento di Fisica dell'Università di Trento, I-38050 Povo (Trento), Italy

Abstract. Tanks to the peculiar sensitivity to correlation of vibrational motion, EXAFS contains original information on thermal properties of crystals. The thermal expansions measured by EXAFS and by Bragg scattering have a different physical meaning. They can be experimentally distinguished by accurate temperature dependent measurements, leading to the evaluation of the perpendicular mean square relative displacement (MSRD). These results, besides giving a deeper insight on the connection between EXAFS and lattice dynamics, open new perspectives for studying the local origin of negative thermal expansion.

Keywords: EXAFS, Lattice dynamics, Thermal expansion
PACS: 61.10.Ht, 61.10.Dp, 63.20.-3, 65.40.De

INTRODUCTION

The effects of atomic thermal vibrations on EXAFS have been, at first, taken into account by a harmonic Debye-Waller factor, corresponding to the parallel mean square relative displacement (MSRD) of absorber *(a)* and back-scatterer *(b)* atoms [1]. The difference between the MSRD measured by EXAFS and the sum of the MSDs of the *a* and *b* atoms measured by Bragg scattering is due to the correlation along the bond direction. The inadequacy of the harmonic approximation was quite early detected [2]. An effective approach for treating anharmonicity in moderately disordered systems was guaranteed by the cumulant expansion method [3, 4].

Recently, the difference between thermal expansions measured by EXAFS and by Bragg scattering, expected on the grounds of theoretical considerations [5, 6, 7], has been experimentally evidenced [8, 9, 10], leading to the possibility of measuring the perpendicular MSRD. These findings can give new insights on the very meaning of EXAFS structural and dynamical parameters, and open interesting perspectives for the study of correlation of vibrational motion. The main applications are the test of lattice dynamical theories and the search for the local origin of negative thermal expansion and some kinds of phase transitions.

Aim of this paper is to give an up-to-date account of the recent advances in EXAFS studies of thermal properties of crystals. Section accounts for the basic differences between structural and dynamical parameters obtainable from EXAFS and Bragg scattering. Section is dedicated to some considerations about cumulants. Section contains a comparison between different data analysis procedures. In Section some recent experimental results are presented and discussed. Section is dedicated to conclusions.

DIFFRACTION AND EXAFS

Let us consider a pair of neighboring atoms *a*, *b* in a crystal. Bragg scattering is sensitive to the three-dimensional distributions of instantaneous positions $\mathbf{r}_a$ and $\mathbf{r}_b$ of the two atoms, and measures the distance between average positions, $R = |\langle \mathbf{r}_b \rangle - \langle \mathbf{r}_a \rangle|$ (Fig. 1, a). For crystals with atoms only in special positions, the temperature variation of the distance δR is proportional to the macroscopic thermal expansion measured by dilatometric techniques. EXAFS, like diffuse scattering, samples the one-dimensional distribution of instantaneous interatomic distances, and measures the average value of the instantaneous distances, $\langle r \rangle = \langle |\mathbf{r}_b - \mathbf{r}_a| \rangle$ (Fig. 1, b). The distances R and $\langle r \rangle$ are in principle different. The difference is due to thermal vibrations perpendicular to the direction of the *a*–*b* bond. One sometimes refers to R and $\langle r \rangle$ as *apparent* and *true* bond lengths, respectively [11].

The difference between Bragg scattering and EXAFS is amenable to the different sensitivity to the correlation of atomic vibrations. The *absolute* thermal ellipsoids determined for every atom by Bragg scattering can be parametrized in terms of three absolute mean square displacements (MSD) along three independent directions. In case of axial symmetry around the *a*–*b* bond direction, only two MSD are sufficient, which can be conveniently chosen as one parallel and one perpendicular to the bond, $U^i_{||}$ and $U^i_{\perp}$, respectively, where $i = a, b$. EXAFS is sensitive to the *relative* displacements of atom *b* with respect to atom *a*, $\Delta\mathbf{u} = \mathbf{u}_b - \mathbf{u}_a$. Again, it is convenient to consider the projection of $\Delta\mathbf{u}$ along the *a*–*b* bond direction and in the perpendicular plane: $\Delta u^2 = \Delta u^2_{||} + \Delta u^2_{\perp}$ [7].

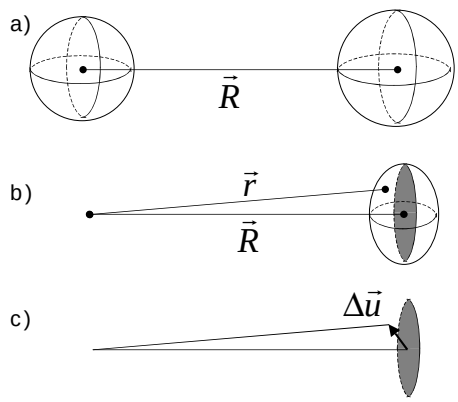

FIGURE 1. Schematic representation of the difference between Bragg diffraction and EXAFS. a) Ellipsoids of absolute atomic thermal motion probed by diffraction. b) Ellipsoid of relative thermal motion probed by EXAFS. c) Relative displacement vector $\Delta\mathbf{u}$.

The *parallel* MSRD $\langle\Delta u_{||}^2\rangle$ can be expressed as [1]

$$\langle\Delta u_{||}^2\rangle = \langle(\hat{\mathbf{R}}\cdot\mathbf{u}_a)^2\rangle + \langle(\hat{\mathbf{R}}\cdot\mathbf{u}_b)^2\rangle - 2\langle(\hat{\mathbf{R}}\cdot\mathbf{u}_a)(\hat{\mathbf{R}}\cdot\mathbf{u}_b)\rangle. \quad (1)$$

The first two terms on the right-hand side of Eq. 1 correspond to the uncorrelated MSDs along the bond direction, $U_{||}^a = \langle(\hat{\mathbf{R}}\cdot\mathbf{u}_a)^2\rangle$ and $U_{||}^b = \langle(\hat{\mathbf{R}}\cdot\mathbf{u}_b)^2\rangle$, respectively. The last term is the *parallel* displacement correlation function (DCF).

The *perpendicular* MSRD $\langle\Delta u_{\perp}^2\rangle$ establishes the connection between the distances measured by EXAFS and by Bragg scattering. One can easily show that, to a good approximation [5, 7],

$$\langle r\rangle = R + \langle\Delta u_{\perp}^2\rangle/2R. \quad (2)$$

To the extent that $\langle\Delta u_{\perp}^2\rangle$ increases with temperature, the thermal expansion measured by EXAFS is larger than the thermal expansion masured by Bragg scattering. From the independent measurements of $\langle r\rangle$ and R, by inversion of Eq. (2) one can obtain the perpendicular MSRD $\langle\Delta u_{\perp}^2\rangle$. In case of axial symmetry around the bond direction, the sum of the uncorrelated MSDs $U_{\perp}^a + U_{\perp}^b$ measured by Bragg scattering can be directly compared with the perpendicular MSRD divided by two, $\langle\Delta u_{\perp}^2\rangle/2$, the residual difference being due to correlation in perpendicular direction.

Although no complete information on correlation can be obtained solely from Bragg scattering, one can show that the minimum and maximum possible values for parallel and perpendicular MSRDs can be calculated from the uncorrelated MSDs [5]:

$$U_{||}^a + U_{||}^b - 2\left(U_{||}^a U_{||}^b\right)^{\frac{1}{2}} \le \langle\Delta u_{||}^2\rangle \le U_{||}^a + U_{||}^b + 2\left(U_{||}^a U_{||}^b\right)^{\frac{1}{2}} \quad (3)$$

$$U_{\perp}^a + U_{\perp}^b - 2\left(U_{\perp}^a U_{\perp}^b\right)^{\frac{1}{2}} \le \frac{\langle\Delta u_{\perp}^2\rangle}{2} \le U_{\perp}^a + U_{\perp}^b + 2\left(U_{\perp}^a U_{\perp}^b\right)^{\frac{1}{2}} \quad (4)$$

The minimum and maximum values correspond to motion of a and b atoms perfectly in phase and in opposition of phase, respectively. If the ellipsoids of the a and b atoms are equal, the minimum values are zero. The difference between the parallel MSRD $\langle\Delta u_{||}^2\rangle$ measured by EXAFS and the minimum possible value obtained from Bragg scattering allows an estimate of the strength of the a–b bond against stretching.

Both parallel and perpendicular MSRDs can be expressed as a function of eigenvectors and eigenvalues of the dynamical matrix. Their temperature dependencies can reasonably by fitted to correlated Einstein or Debye models [12]. Only in the case of perfect isotropy, however, are the Einstein or Debye frequencies of parallel and perpendicular MSRDs equal, and the ratio $\gamma = \langle\Delta u_{\perp}^2\rangle/\langle\Delta u_{||}^2\rangle = 2$. Actually, relative atomic vibrations can never be *a priori* considered perfectly isotropic, neither for simple metals. As a consequence, the ratio $\gamma = \langle\Delta u_{\perp}^2\rangle/\langle\Delta u_{||}^2\rangle$ is generally temperature dependent, and its values can be, for some crystals, much higher than two. An accurate evaluation of $\langle r\rangle$ from R, or viceversa, is thus impossible without a detailed independent knowledge of $\langle\Delta u_{\perp}^2\rangle$, e.g. from lattice dynamical calculations.

At last, no *a priori* relations can be established between the shapes of absolute Bragg ellipsoids and of relative EXAFS ellipsoids. The EXAFS ellipsoids are generally anisotropic ($\gamma > 2$), also when Bragg ellipsoids are spherical (see below).

DISTRIBUTION AND CUMULANTS

For a crystal lacking structural disorder, an EXAFS spectrum samples a canonical distribution of interatomic distances. For the sake of simplicity, let us focus here on the single scattering path corresponding to a well isolated coordination shell. The canonical average can be expressed in real space as the integral over a one-dimensional distribution of distances [13, 14],

$$\chi(k) \propto \left\langle \frac{e^{-2r/\lambda(k)}}{r^2} e^{2ikr} \right\rangle = \int_0^{\infty} P[r,\lambda(k)] e^{2ikr} dr, \quad (5)$$

where

$$P[r,\lambda(k)] = \rho(r)\, e^{-2r/\lambda(k)}/r^2 \quad (6)$$

is referred to as *effective* distribution [3], $\rho(r)$ being the *real* distribution. For moderately disordered systems, the distributions $\rho(r)$ and $P[r,\lambda(k)]$ can be parametrized in terms of their cumulants, C_1^* and C_i, respectively. The first cumulant $C_1^* = \langle r\rangle$ is the average value of the distribution $\rho(r)$. The second cumulant is the variance of the

distribution, and corresponds, to a good approximation, to the parallel MSRD, $C_2^* = \langle \Delta u_{||}^2 \rangle$. The third cumulant measures the asymmetry of the distribution. In general, one can assume $C_i^* = C_i$ for $i > 1$, while for $i = 1$

$$C_1^* = C_1 + 2C_2[1/C_1 + 1/\lambda(k)]. \quad (7)$$

The connection between EXAFS cumulants and force constant of the interaction potential has been thoroughly investigated for the case of a two-atomic system, leading to parametrized expressions of the first cumulants as a function of temperature [15, 16]. For a two-atomic system, the termal expansion measured by the first cumulant is solely due to the asymmetry of the interaction potential. It can thus be independently obtained also from the values of the second and third cumulants, and corresponds to $a = -3k_3C_2^*/k_0$, where k_0 and k_3 are the 2nd and 3rd-order force constants, respectively [15].

For a crystal, the potential is defined within a 3N-dimensional configurational space. The connection between the crystal potential and the one-dimensional EXAFS distribution of distances and its effective potential is far from trivial. While the true bond thermal expansion is still measured by the temperature variation of the first cumulant, there is no *a priori* relation between thermal expansion and third cumulant, so that in general the quantity $a = -3k_3C_2^*/k_0$ cannot be considered a measure of thermal expansion. The one-dimensional EXAFS effective potential for a crystal is in principle temperature dependent, both in position and shape. Experimental evidence seems to exclude relevant shape variations, while a shift of the minimum position has been observed for all investigated systems. The thermal expansion (first cumulant) is thus a joint effect of asymmetry (third cumulant) and shift of the effective potential. A relevant contribution to the potential shift is related to vibrations perpendicular to the bond [4].

DATA ANALYSIS

Two different approaches to data analysis are possible when information on thermal properties of crystals is sought: the first one *(phenomenological)* is based on the so-called *ratio method* [3], using the lowest temperature spectrum as reference for scattering amplitudes, phase-shifts and inelastic terms; the second one *(theoretical)* is based on the simulation of the EXAFS signal by suitable computer codes, like FEFF [17], and the determination of the structural and dynamical parameters by non linear best fit to the experimental signal.

The phenomenological method is suitable only for well isolated first-shells, where no multiple scattering effects are expected. Its main advantages are the lack of theoretical inputs, the disentanglement of phase and amplitude parameters and the possibility of estimating, by simple visual inspection, the quality of experimental data and the possible residual correlation effects between parameters. The results of the analysis are the relative values ΔC_i of the cumulants of the effective distribution. A disadvantage of the method is the difficulty of taking into account the k-dependence of the mean free path, which introduces an uncertainty in the evaluation of C_1^* through Eq. (7). The theoretical method is in principle applicable to both single and multiple scattering paths, and can take into account the k-dependence of λ. It can directly give absolute values of the cumulants C_i^* of the real distribution. On the other hand, the accuracy of results depends on the reliability of theoretical models. Besides, there is a less immediate control of the quality of experimental data. In general, the recommended choice is the utilization of both methods, when applicable, and a critical comparison of their results.

EXPERIMENTAL RESULTS

Temperature-dependent EXAFS measurements have been recently performed on several different systems, to check the sensitivity of EXAFS to their thermal properties. In general, very accurate relative values of the first three cumulants could be obtained for the first shell, with a good agreement between the phenomenological and theoretical procedures of data analysis. For all the crystals studied, the thermal expansion δC_1^* measured by EXAFS was unambiguously larger than the crystallographic thermal expansion δR, and different from the thermal expansion solely determined by the asymmetry of the effective potential, $a = -3k_3C_2^*/k_0$. A check of self-consistency of the data analysis procedures was considered the good agreement of the temperature dependence of the third cumulant with the theoretical behaviour expected according to the perturbative quantum approach of Refs. [15, 16].

When using the phenomenological approach, absolute values of parallel and perpendicular MSRDs were obtained by fitting suitable Einstein or Debye models [12] to their relative values. The so obtained absolute values of the parallel MSRD are generally in agreement with the values determined through the theoretical approach. The ratio $\gamma = \langle \Delta u_{\perp}^2 \rangle / \langle \Delta u_{||}^2 \rangle$ has been used to measure the anisotropy of relative thermal vibrations ($\gamma = 2$, independent of temperature, in case of perfect isotropy).

The contribution to EXAFS of outer shells has always been analyzed by the theoretical approach, taking into account multiple scattering contributions. Less accurate results could however be obtained than for the first shell, in particular concerning thermal expansion and third cumulant.

Let us now consider in more details the results obtained for different systems.

Copper

In the case of copper [10], the results for the first shell show that a resolution better that 0.001 Å can be achieved for the relative values of interatomic distances. The thermal expansion coefficients α determined from the first EXAFS cumulant δC_1^* and from the asymmetry of the distribution (parameter a) are compared in Table 1 with the crystallographic thermal expansion. The positive difference $\alpha[C_1^*] - \alpha[R]$ is due to the effect of perpendicular vibrations, and corresponds to a positive shift of the effective potential [4]. The larger difference $\alpha[C_1^*] - \alpha[a]$ corresponds to a total positive shift of the effective potential larger than expected as a sole effect of perpendicular vibrations, and shows that the parameter a does not measure nor the EXAFS nor the crystallographic thermal expansion. The difference $\delta C_1^* - \delta R$ has allowed us to evaluate the temperature dependence of the perpendicular MSRD. The temperature dependence of the first-shell parallel MSRD is well fitted to a correlated Debye model with the same Debye temperature as specific heats and diffraction Debye-Waller factor. The Debye temperature of the perpendicular MSRD is however slightly lower, indicating a slight anisotropy of relative vibrational motion, which is quantified by the ratio γ, asymptotically larger than 2 at high temperature (Table 1). The temperature dependence of the first shell parameters determined experimentally (average distance, parallel and perpendicular MSRDs, third cumulant) were satisfactorily reproduced by path-integral Monte Carlo calculations [18] where, at each temperature, the lattice parameter was adjusted to account for crystallographic thermal expansion.

For the first three outer shells, only a unique average thermal expansion could be reasonably obtained by a non-linear best fit procedure taking into account multiple scattering effects. Meaningful values of parallel MSRDs could instead be obtained separately for each shell. When fitted to correlated Debye models, the MSRDs of third and fourth shell have the same Debye temperature as the first shell, while the Debye temperature of the second shell is lower, indicating a lower degree of correlation, in agreement with recent calculations for fcc metals [19].

Germanium

Also for the first shell of germanium [9] the coefficient of thermal expansion measured by EXAFS is larger than the one measured by diffraction (Table 1), and does not correspond to the coefficient solely due to the effective potential asymmetry. The perpendicular MSRD is much larger than the parallel MSRD, indicating a non-negligible anisotropy of the relative vibrations (asymptotically, $\gamma \simeq 6$), in spite of the isotropy of absolute atomic vibrations measured by Bragg scattering. Beyond the first shell, reliable values could be obtained only for the parallel MSRD of second and third shell. The inadequacy of the correlated Debye model for fitting the MSRDs with a unique temperature is clearly demonstrated, the correlation effect for the first shell being much stronger than expected according to the Debye model [20]. The experimental values of the parallel and perpendicular MSRDs and of the third cumulant of the germanium first shell have been well reproduced by ab-initio dynamical calculations, including a perturbative treatment of anharmonicity [21].

TABLE 1. Coefficients of thermal expansion $\alpha \times 10^5$ at 300 K of the first EXAFS cumulant C_1^*, of the crystallographic distance R and from the asymmetry of the effective potential (a). The last column gives the asymptotic value of the ratio $\gamma = \langle \Delta u_\perp^2 \rangle / \langle \Delta u_{||}^2 \rangle$.

	$\alpha[C_1^*]$	$\alpha[R]$	$\alpha[a]$	$\gamma(\infty)$
Cu	2.2±0.1	1.6	1.3±0.1	2.5±0.3
Ge	1.2±0.1	0.6	0.6±0.1	6±0.3
AgI	1.7±0.5	0±0.2	3.5±0.5	6±1

Silver iodide

In β-AgI, both the pioneering study based on the excluded volume model [22] and the study based on the cumulant approach [23] agree in detecting a strong correlation effect in the parallel MSRD of the I–Ag first shell distribution. The large difference found between the EXAFS and diffraction thermal expansions [8] is however consistent with a perpendicular MSRD much larger than the parallel MSRD (Table 1). It is the large relative motion perpendicular to the I–Ag bond that is probably responsible for the onset of the superionic phase transition at 420 K. The negative difference $\alpha[C_1^*] - \alpha[a]$ suggests an overall negative shift of the effective potential.

Negative thermal expansion materials

Several crystals are affected by isotropic negative thermal expansion (NTE) [11]. In many of these systems, the macroscopic expansion results from the competition between a positive contribution due to bond stretching and a negative contribution due to a tension effect. The tension effect is often amenable to vibrations perpendicular to some inter-atomic bonds, giving rise to a 'guitar-string' effect; it is the case of systems with the diamond and zincblende structure, like germanium or CuCl, where NTE is generally limited to a narrow temperature interval. NTE can extend over very large temperature intervals in framework structures made up by networks

of polyhedral structural units connected by corners, like ZrW_2O_8 [24], Ag_2O [25], $Zn(CN)_2$ [26]. NTE has often been attributed to low-frequency rigid unit modes (RUMs) [27], although no definite correlation between RUMs and NTE can be established for all framework structures [28].

The ability of measuring the true thermal expansion of selected bonds, as well as both parallel and perpendicular MSRDs, makes EXAFS a powerful tool for investigating the local origin of negative thermal expansion. In addition to the work on germanium [9], where NTE is anyway very weak, a thorough study, based on a joint approach EXAFS + diffraction, has been recently done on Cu_2O and Ag_2O [29]. A further investigation is under way on CuCl. The results up to now obtained can be summarized as follows: *a)* The nearest-neighbour distance always undergoes positive expansion. *b)* NTE is better correlated to the anisotropy of relative vibrations measured by EXAFS than of absolute vibrations measured by Bragg diffraction. *c)* The analysis of outer shells can give relevant information; in the case of Cu_2O and Ag_2O EXAFS results suggest the presence of a rather complex dynamical behaviour, inconsistent with RUM models.

CONCLUSIONS

a) A non negligible difference exists between distances and thermal expansions measured by EXAFS and by Bragg scattering. The difference has a well defined physical meaning, and can be exploited to obtain the perpendicular MSRD and to evaluate the anisotropy of relative thermal vibrations.

b) No accurate information on thermal expansion can be obtained from the third cumulant, since the effective EXAFS pair potential depends on temperature.

c) The reproduction of parallel and perpendicular MSRD is a unique test for the phase relationships between eigenvectors of the dynamical matrix obtained from *ab-initio* or model calculations.

d) Sensitivity to the true bond distance and to perpendicular vibrations can be effectively exploited to investigate on the local origin of negative thermal expansion.

ACKNOWLEDGMENTS

The author is indebted to people who collaborate with him in EXAFS studies of thermal properties of crystals: G. Dalba, R. Grisenti, F. Rocca, A. Sanson, M. Vaccari, J. Purans, A. Kuzmin, S. a Beccara, and D. Diop.

REFERENCES

1. G. Beni, and P. M. Platzman, *Phys. Rev. B* **14**, 1514–1518 (1976).
2. P. Eisenberger, and G. S. Brown, *Solid St. Commun.* **29**, 481–484 (1979).
3. G. Bunker, *Nucl. Instrum. Methods Phys. Res.* **207**, 437–444 (1983).
4. P. Fornasini, F. Monti, and A. Sanson, *J. Synchrotron Radiat.* **8**, 1214–1220 (2001).
5. W. R. Busing, and H. A. Levy, *Acta Cryst.* **17**, 142–146 (1963).
6. B. T. M. Willis, and A. W. Pryor, *Thermal Vibrations in Crystallography*, Cambridge University Press, 1975.
7. P. Fornasini, *J. Phys.: Condens. Matter* **13**, 7859–7872 (2001).
8. G. Dalba, P. Fornasini, R. Gotter, and F. Rocca, *Phys. Rev. B* **52**, 149–157 (1995).
9. G. Dalba, P. Fornasini, R. Grisenti, and J. Purans, *Phys. Rev. Lett.* **82**, 4240–4243 (1999).
10. P. Fornasini, S. a Beccara, G. Dalba, R. Grisenti, A. Sanson, M. Vaccari, and F. Rocca, *Phys. Rev. B* **70**, 174301 (2004).
11. G. D. Barrera, J. A. Bruno, T. H. K. Barron, and N. L. Allan, *J. Phys.: Condens. Matter* **17**, R217–R252 (2005).
12. M. Vaccari, and P. Fornasini, *J. Synchrotron Rad.* **13**, 321–325 (2006).
13. E. A. Stern, D. E. Sayers, and F. W. Lytle, *Phys. Rev. B* **11**, 4836–4846 (1975).
14. M. Vaccari, and P. Fornasini, *Phys. Rev. B* **72**, 092301 (2005).
15. A. I. Frenkel, and J. J. Rehr, *Phys. Rev. B* **48**, 585–588 (1993).
16. T. Yokoyama, *J. Synchrotron Rad.* **6**, 323–325 (1999).
17. A. Ankudinov, B. Ravel, J. Rehr, and S. Conradson, *Phys. Rev. B* **58**, 7565 (1998).
18. S. a Beccara, G. Dalba, P. Fornasini, R. Grisenti, F. Pederiva, A. Sanson, D. Diop, and F. Rocca, *Phys. Rev. B* **68**, 140301 (2003).
19. I. K. Jeong, R. H. Heffner, M. J. Graf, and S. J. L. Billinge, *Phys. Rev. B* **67**, 104301 (2003).
20. G. Dalba, and P. Fornasini, *J. Synchrotron Radiat.* **4**, 243–255 (1997).
21. G. Birner, D. Strauch, and P. Pavone (2001), private commun.
22. J. B. Boyce, T. M. Hayes, and J. C. Mikkelsen, Jr, *Phys. Rev. B* **23**, 2876–2896 (1981).
23. G. Dalba, P. Fornasini, F. Rocca, and S. Mobilio, *Phys. Rev. B* **41**, 9668–9675 (1990).
24. T. A. Mary, J. S. O. Evans, T. Vogt, and A. W. Sleight, *Science* **272**, 90–92 (1996).
25. W. Tiano, M. Dapiaggi, and G. Artioli, *J. Appl. Cryst.* **36**, 1461–1463 (2003).
26. K. W. Chapman, P. J. Chupas, and C. J. Kepert, *J. Am. Chem. Soc.* **127**, 15630–15636 (2005).
27. V. Heine, P. R. L. Welche, and M. T. Dove, *J. Am. Ceram. Soc.* **82**, 1793–1802 (1999).
28. J. Tao, and A. Sleight, *J. Solid St. Chem.* **173**, 442–448 (2003).
29. A. Sanson, F. Rocca, G. Dalba, P. Fornasini, R. Grisenti, M. Dapiaggi, and G. Artioli, *Phys. Rev. B* **73**, 214305 (2006).